

# Automatic Computation of Biophysical Cell Parameters in Digital Holographic Microscopy Images

Lilith Brandt<sup>1</sup>, Klaus Brinker<sup>1</sup> and Björn Kemper<sup>2</sup>

<sup>1</sup>Hamm-Lippstadt University of Applied Sciences, Marker Allee 76-78, Hamm, Germany

<sup>2</sup>Biomedical Technology Center, University of Münster, Mendelstraße 17, Münster, Germany

**Keywords:** Computer Vision, Segmentation, Region Detection, Digital Holographic Microscopy, Quantitative Phase Imaging, Automatic Cell Detection.

**Abstract:** This paper presents an analysis pipeline for automatically detecting cells in digitally reconstructed quantitative phase images acquired by digital holographic microscopy and for computing biophysical cell parameters. Using an intelligent, integrated image analysis approach, we optimize the overall analysis process which includes several time-consuming, manual steps. The proposed automatic approach shows promising results in an experimental comparison with the current manual evaluation process.

## 1 INTRODUCTION

Quantitative phase images acquired by a digital holographic microscopy (DHM) can be used for the analysis of biological cells, e.g. measuring their reaction to drugs or nanoparticles. Quantitative phase contrast methods provide contactless, minimally-invasive imaging and thus examined cells are not altered, e.g., by fluorescent dyes. Due to the numerical reconstruction of quantitative phase images it is possible to determine biophysical parameters such as cell volume, dry mass and refractive index numerically (Kemper et al., 2013).

The analysis of cells in digital quantitative phase images typically involves several time-consuming steps in the processing pipeline: In order to compute biophysical cell parameters with high accuracy and reliability, as described for example in (Kastl et al., 2017), single cells are manually selected in a hologram, individually reconstructed and the physical cell parameters are separately determined via different software packages. A fast automated evaluation of a sufficient number of images for further statistical analysis with an adequate precision is currently not possible. Modern image processing and analysis provides techniques to automatically detect cells in microscopy images, which therefore allow removing the conventional time-consuming approach to manually select cells in quantitative phase images. In addition, digital image processing

allows both, to compute morphological parameters of cells, and conduct automatic cell identification.

Therefore, this paper presents a pipeline for automatically detecting appropriate cells in reconstructed quantitative phase images that is combined with an all-in-one computation of cell-specific biophysical parameters in order to optimize the overall time-consumption of the analysis process.

First, an introduction in digital holographic microscopy and the possibilities of computing cell physical parameters from quantitative phase images is given in sections 2.1 and 2.2. Then, for detecting individual cells in 2D reconstructed phase images, we present a suitable image segmentation concept. Based on the cell segmentation individual biophysical parameters such as dry mass and cell volume are determined for each cell automatically. We elaborate on this analysis step with more details in section 2.3. In section 3, we present experimental results from comparing our novel approach with the current manual evaluation process. Finally, conclusions are drawn in section 4.

## 2 METHOD & IMPLEMENTATION

In this section the underlying digital holographic microscopy (DHM) principle and the computation of biophysical cell parameters from quantitative phase images taken by DHM are described. In order to

accomplish the automatic computation the last subsection will deal with the required techniques of digital image processing, in particular with the segmentation and object recognition methods used for cell detection in this paper.

## 2.1 Digital Holographic Microscopy

Digital holographic microscopy is a method which is based on the classical principle of holography, where both the amplitude and the phase of light waves are stored and reconstructed to produce spatial images of an object. The principle of holography was introduced by physicist Dennis Gabor in 1948 (Gabor, 1948). Based on the wave theory of light, it is assumed that the light propagates in a wavelike manner with a specific wavelength, amplitude and phase. For recording a hologram, light from a laser is divided by a beam splitter into a reference wave and an object wave. In the case of transillumination, depending on the optical and geometric properties of the sample, the phase of the object wave changes.

The object is transmitted by the object wave and then interferes with the undisturbed reference wave. Due to the interference with the reference wave, an interference pattern is formed. In contrast to classical analog holography, in digital holography (DH) the hologram is not recorded with a photo plate and again illuminated with the reference wave for optical reconstruction. Instead, a charge coupled device

(CCD) sensor is used, which digitizes the intensity of the interference pattern (digital hologram). The digital hologram thus contains beside the amplitude also the information of the phase of the object wave, which can be digitally reconstructed (Kemper and von Bally, 2008).

Figure 1 shows the setup for digital holographic phase contrast microscopy used in this study to produce digital holograms (Kemper et al., 2006). Holograms are recorded with an inverted microscope iMIC (TILL Photonics GmbH, Munich, Germany) modified for digital holographic microscopy. A frequency-doubled neodymium: yttrium aluminium garnet laser, Compass 315M-100 (Coherent GmbH) with a wavelength of  $\lambda = 532 \text{ nm}$  is used as the coherent light source. A CCD camera, (DMK 41ABF02, The Imaging Source, Bremen, Germany) and a 10x microscope objective are used for imaging of the sample and to record the digital holograms. The resulting digital holograms are transferred to a computer for numerical reconstruction. The numerical reconstruction from the digitally captured holograms is performed by spatial phase shifting in combination with optional numerical autofocusing (Langehanenberg et al. 2011).

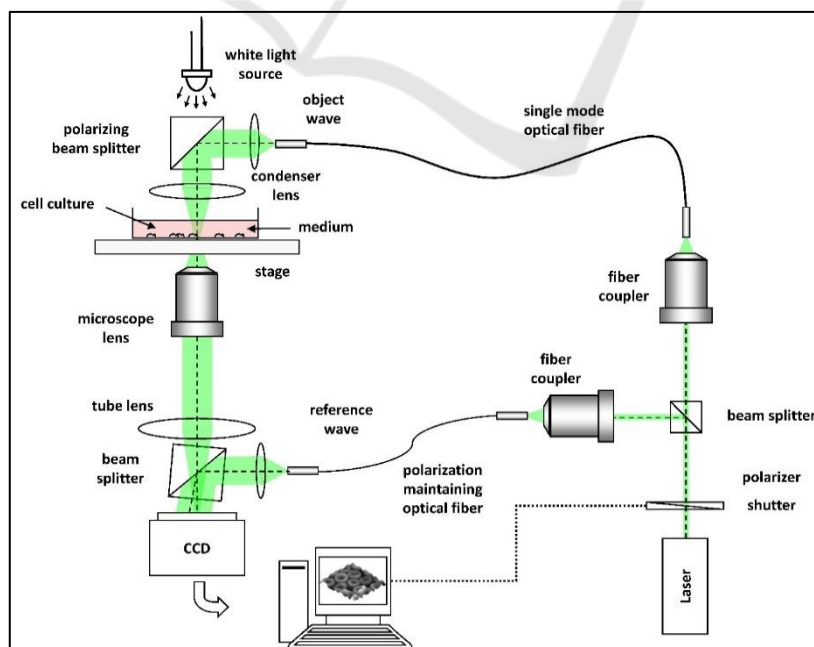


Figure 1: Digital holographic microscopy set up (adapted from Kemper et al. 2013).

## 2.2 Computation of Biophysical Cell Parameters from Quantitative DHM Phase Images

In this section we describe how from the measured optical pathlength changes in the reconstructed quantitative phase contrast images of suspended cells biophysical cell parameters can be determined (Kemper et al., 2013).

### 2.2.1 Cell Volume

We assume that the considered cells observed in suspension are approximately spherical. Hence, the cross section of the cell surface  $S_c$  is detected as a circle, the cell radius  $r_{cell}$  can be easily calculated:

$$S_c = \pi \cdot r_{cell}^2. \quad (1)$$

The detected pixel area has to be converted into the metric units of the surface area  $S_c$  of the cell in  $\mu m^2$  using the respective scaling factor of the microscope objective. Since the cells are assumed to be spherical, the cell volume  $V$  is:

$$V = \frac{4}{3} \pi r_{cell}^3. \quad (2)$$

### 2.2.2 Dry Mass

The dry mass is defined as the amount of all substances dissolved in the cell except water. By utilizing the projected cell surface area  $S_c$  and the average phase contrast  $\Delta\bar{\varphi}$ , the cellular dry mass  $DM$  is computed as (Kastl et al., 2017):

$$DM = \frac{10\lambda}{2\pi\gamma} \Delta\bar{\varphi} S_c. \quad (3)$$

The parameter  $\lambda$  represents the wavelength of the laser light in  $\mu m$ ,  $S_c$  the cross section area in  $\mu m^2$ ,  $\Delta\bar{\varphi}$  the mean phase difference induced by the cell, and  $\gamma$  a specific constant related to the cellular content (refractive index increment) (Barer, 1952). Following (Kastl et al., 2017), the value of  $\gamma$  is estimated as  $0.002 m^3 / kg$  in this work. The mean phase contrast  $\Delta\bar{\varphi}$  can be calculated by averaging all phase values of a quantitative digital holographic phase contrast image of a cell. The respective phase contrast values are calculated from the reconstructed phase contrast image, which is represented in grey levels (8-bit), by normalizing the intensity of the grey values and multiplying by the maximum phase contrast value in the image.

### 2.2.3 Refractive Index

The refractive index is a material specific parameter, which quantifies how much the light is delayed while passing through the sample. It is proportional to the concentration of the substances dissolved in the cell. The change in phase contrast  $\Delta\bar{\varphi}$  depends on the refractive index of the cell  $\eta_{cell}$ , refractive index of the surrounding medium  $\eta_{medium}$ , and the cell thickness  $\bar{d}_{cell}$ :

$$\Delta\bar{\varphi} = \frac{2\pi}{\lambda} \bar{d}_{cell} \cdot (\eta_{cell} - \eta_{medium}). \quad (4)$$

Using the assumption of a spherical cell shape, by equations (1), (3), (4) and taking a mean cell thickness  $\bar{d}_{cell} = \frac{V}{S_c}$  into account, the dry mass  $DM$  evaluates to (Kastl et al. 2017):

$$DM = 10 \frac{V}{\gamma} (\eta_{cell} - \eta_{medium}). \quad (5)$$

From equation (5) the cellular refractive index of  $\eta_{cell}$  can be calculated

$$\eta_{cell} = \frac{DM \cdot \gamma + 10 \cdot V \cdot \eta_{medium}}{10 V}. \quad (6)$$

Equation (6) shows that that  $\eta_{cell}$  is an optical parameter that is directly related to cell volume and dry mass.

## 2.3 Automatic Cell Detection

To accomplish the tasks of detecting individual cells automatically and determine their biophysical cell parameters from the reconstructed digital holographic phase images, several pre-processing steps are required. These steps will be discussed in more detail in the following subsections.

### 2.3.1 Image Segmentation

The numerically reconstructed images of cells need to be segmented, in order to subsequently mark the cells as contiguous regions. Several pre-processing steps are carried out in order to obtain an optimal segmentation result. First, we smoothed the image with a median filter. The aim here is to eliminate unevenness in the phase distributions, but at the same time preserve the important image structures. In order to make a precise distinction between the foreground and the background during thresholding and to account for possible image artefacts, we used the background subtraction technique. More precisely, we employed a large Gaussian filter ( $\sigma = 200$ ) in order to generate a strongly smoothed image which

serves as an approximate model for the image background.

By subtracting the generated background reference image, light background patterns (fixed pattern noise) can be eliminated in the quantitative phase image and the resulting images can be effectively segmented. The threshold value is calculated with the threshold method according to Otsu to create a binary image (Otsu, 1979). It is assumed that the pixels of the original grey-scale image originate from two classes whose distribution is not known. The threshold value is determined in such a way that the dispersion of the grey values, i.e. the variance within a class is as small as possible and the mean value between the two classes is simultaneously as far apart as possible (Burger and Burge, 2009).

### 2.3.2 Region Detection

After the segmentation, the detection of connected objects, in this case the recognition of individual areas as one cell, is required in order to calculate the individual biophysical cell parameters. For this purpose, we used simple flood filling to label each connected region in the binary image. Based on a labelled image a variety of parameters for each region such as geometric features as well as intensity-based information can be computed.

## 2.4 Implementation

The steps described in the previous section were developed and implemented in Python. In this work, the Python version 3.6.1 was used. In addition to the standard library of Python, for the basic handling of images, functions from the libraries NumPy and Pillow were used. In our pipeline the scikit-image library has been used for object recognition and for determining the cell parameters. Scikit-image provides a collection of algorithms for image processing and computer vision. We used the version 0.13.0 by scikit-image, in particular, functions from the sub-packs feature, filters, and morphology.

## 3 EXPERIMENTAL RESULTS

We applied our pipeline to several different reconstructed DHM quantitative phase images to analyse the performance of automatically detecting different cell types. The pipeline detected all cells as shown in Figure 2 (a) and Figure 3.

In order to evaluate how the data acquired with the described automatic detection differs from the values determined with manual detection, the specific biophysical parameters were computed and compared for both approaches.

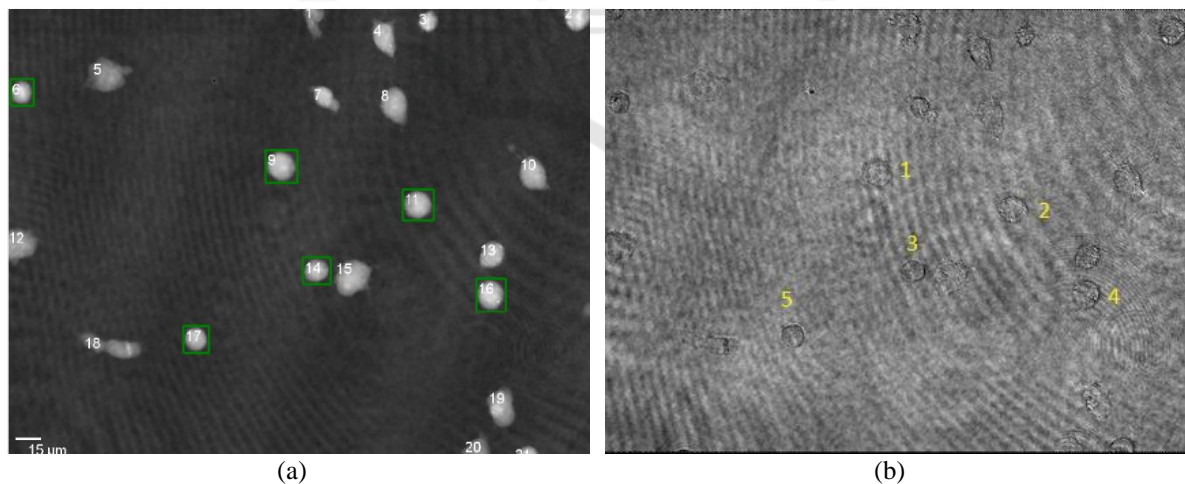


Figure 2: (a) shows the cells detected automatically in a quantitative DHM phase contrast image. The green boxes mark cells with a form factor  $> 0.88$ . (b) shows the corresponding cells manually selected cells in the associated amplitude image.

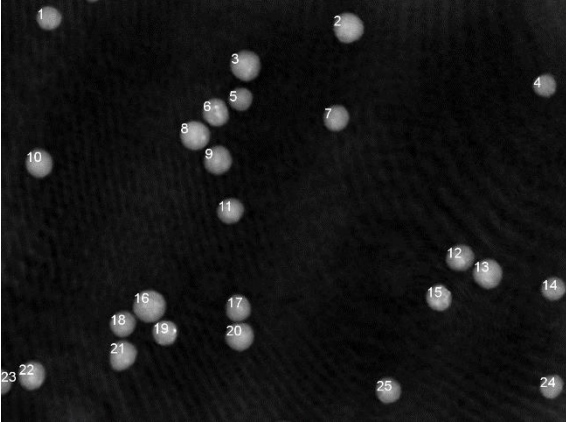


Figure 3: Detected and labelled cells in quantitative DHM phase contrast images of suspended PaTu 8988T cells using the developed pipeline.

Using an image series of ten quantitative phase contrast images of suspended pancreatic tumour cells (PaTu 8988T) and literature values from (Kastl et al., 2017) the accuracy of the pipeline was analysed. In the image series, a total number of 254 cells were automatically detected and 189 cells with a form factor higher than 0.88 were further evaluated for biophysical parameters. The cells which were used were marked with a green bounding box (Figure 2). The statistical results can be represented as follows:

Table 1: Radius, refractive index and dry mass retrieved from 189 automatically detected PaTu 8988T cells.

	Mean	Minimum	Maximum	Standard Deviation
Radius [ $\mu\text{m}$ ]	$7.4768 \pm 0.0581$	5.6998	10.0785	0.7976
Dry mass [ng]	$0.234 \pm 0.006$	0.0764	0.6097	0.0826
Ref. index	$1.3637 \pm 0.0001$	1.3637	1.3693	0.0001

For the PaTu 8988T cells, a refractive index of  $\eta_{\text{cells PaTu 8988T}} = 1.3637 \pm 0.0001$  and a radius of  $R_{\text{cells PaTu 8988T}} = 7.48 \pm 0.058$  were determined using the described pipeline. Literature values specified in (Kastl et al., 2017) for the refractive index for the PaTu 8988T cells are  $\eta_{\text{cells PaTu 8988T}} = 1.3654 \pm 0.0002$  and for the radius

$R_{\text{cells PaTu 8988T}} = 8.7 \pm 0.006$ . The comparison of the mean cell radii of the two measurement series shows that the results from the pipeline are significantly smaller than the literature value, which leads to an underestimation of the actual dry mass.

In order to obtain a more accurate comparison of the specific biophysical parameters, a further analysis was carried out to evaluate the differences in more detail. The biophysical cell parameters were determined from five different phase contrast images.

Therefore, each reasonable cell in the region of interest was detected manually by a person. Then an individual phase image of the region was reconstructed from the hologram and the parameters were calculated manually with different software components. A total number of 26 cells were included in the evaluation. The identical cells were automatically detected in overall reconstructed phase contrast images of all cells.

Compared to the manual method, the process of the automatic analysis is many times faster. The whole quantitative phase contrast image is evaluated at once rather than individually selecting and reconstructing each cell and conducting further analysis steps.

The direct comparison of the calculated parameters, shows that the radius and dry mass of the cells determined after automatically detecting them shows the same tendency but are lower than manually determined values.

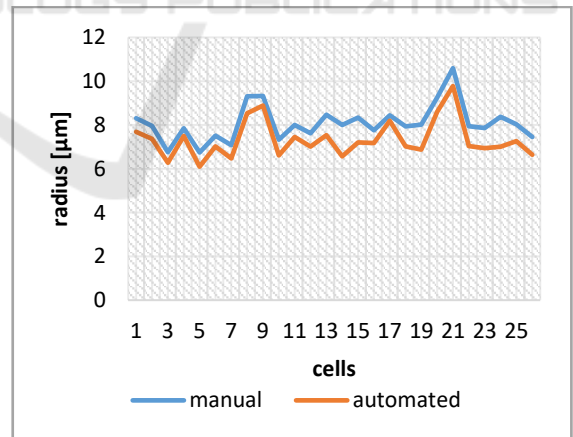


Figure 4: Comparison of the radii of 26 PaTu 8988T cells determined in by automatic evaluation and manual detection.

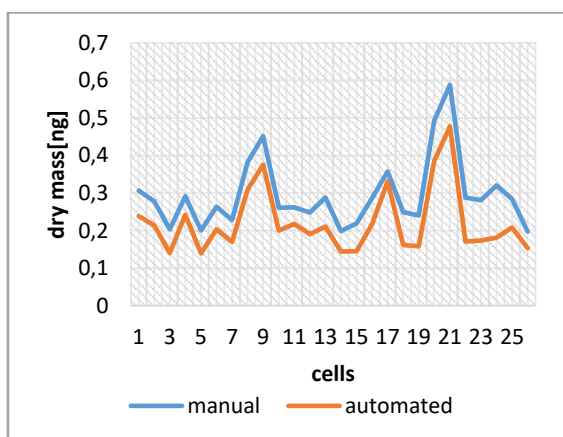


Figure 4: Comparison of the dry mass of 26 PaTu 8988T cells determined by automated evaluation and manual detection.

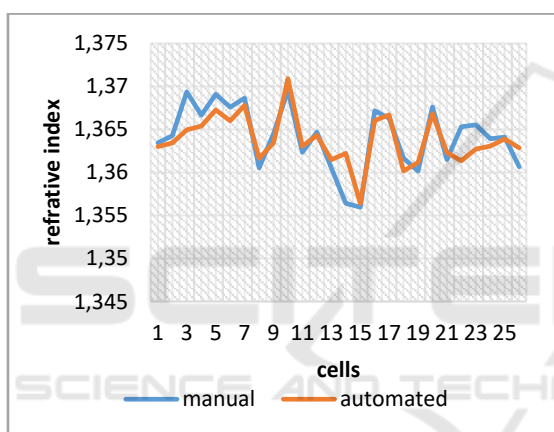


Figure 5: Comparison of the refractive indices of 26 PaTu 8988T cells determined by automated evaluation and manual detection.

When comparing the quantitative phase images of an individual cell with the corresponding binary image (Figure 6), it becomes obvious that the Otsu segmentation method used in our approach and the pre-processing steps do not completely assign the outer edge regions to the cells. Since the edge region has no sharp edge structure, the segmentation process is challenging. As a result, the cells are detected with a smaller area than the real surface, which leads to deviations of the biophysical parameters.

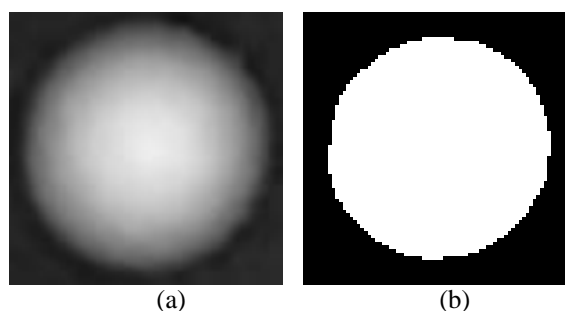


Figure 6: Image sections of an individual cell. (a) shows the original quantitative phase image. (b) shows the corresponding segmented image section.

The cell radius and the dry mass are both dependent on the detected pixel area, which depends on the segmentation result of the image. Overall, the cell radii are about 9.2% smaller than calculated after individual manually detection, which leads to a smaller estimated dry mass of the cells.

## 4 CONCLUSIONS

This paper presents an approach for automatically detecting cells in quantitative digital-holographic phase-contrast images and for determining their cell-specific biophysical parameters using digital image processing and analysis. The biophysical parameters accessible by quantitative phase contrast microscopy, i.e., cell size, cell volume, dry mass and refractive index, were determined automatically in reconstructed images of several cells that were observed in the suspension. The proposed processing pipeline allows to conduct a fully automated detection and calculation of the cell parameters, which simplifies the process compared to detecting them manually for the measurement of individual cells. This pipeline reduces the time complexity by a computer added process optimization, which offers a significantly increased throughput in the evaluation of individual cells. The results in section 4 show that automated detection of suitable cells by using their form factor and calculation of the cell-specific biophysical parameters is possible. However, the direct comparison with results from the manual evaluation of individual cells indicates that the detected cell surfaces exhibit deviations due to the segmentation process used. Therefore, the calculated parameters for cell radius, cell volume and dry mass are lower than expected. For this reason, further research is required to optimize the segmentation process. In addition, further systematic investigations should be carried out on functional testing, as well as

on possible correction factors. In summary, the developed pipeline represents a promising alternative to the current evaluation process of the cells. In particular, the automated detection and the time reduction are an important advantage with regard to the significant increase of measured data. The errors caused by underestimated cell areas during the segmentation have to be improved in the future in order to enable a more accurate retrieval of the biophysical cell parameters. Moreover, in addition to a quantitative evaluation of suitable segmentation methods for cross section image reconstructions, it seems to be promising to consider more advanced segmentation approaches which incorporate the special structure of holographic image data for cell boundary detection.

## REFERENCES

- Barer, R., 1952, *Interference Microscopy and Mass Determination*, Nature 1952; 169:366-367.
- Burger, W., Burge, M. J., 2009, *Principles of Digital Image Processing: Core Algorithms*. Springer.
- Gabor, D., 1948, *A New Microscopic Principle*, In Nature Vol.161, .777-778.
- Kastl, L., Isbach, M., Dirksen, D., Schnekenburger, J., Kemper, B. 2017, *Quantitative Phase Imaging for Cell Culture Quality Control*, Wiley Online Library (DOI 10.1002/cyto.a.23082).
- Kemper, B., Carl, D., Höink, A., von Bally, G., Bredebusch, I., Schnekenburger, J., 2006. *Modular Digital Holographic Microscopy System for Marker Free Quantitative Phase Contrast Imaging of Living Cells*, Proc. SPIE 6191, 61910T.
- Kemper, B., Langehanenberg, P., Kosmeier, S., Schlichthaber, F., Remmersmann, C., Von Bally, G., Rommel, C., Dierker, C., Schnekenburger, J., 2013. *Quantitative Phase Imaging with Digital Holographic Microscopy and Applications in Live Cell analysis*. In Tuchin (Ed.), *Handbook of Coherent-Domain Optical Methods*, Springer 215-257.
- Kemper, B., von Bally, G., 2008. *Digital Holographic Microscopy for Life Cell Applications and Technical Inspection*, Appl. Opt. 47, A52-A61.
- Langehanenberg P, von Bally G, Kemper B., 2011. *Autofocusing in Digital Holographic Microscopy*. 3D Res 2011; 2:1–11.
- Lenz, P., Brückner, M., Ketelhut, S., Heidemann, J., Kemper, B., Bettenworth, D., 2016, *Multimodal Quantitative Phase Imaging with Digital Holographic Microscopy Accurately Assesses Intestinal Inflammation and Epithelial Wound Healing*, JOVE e54460.
- Otsu, N., 1979. *A Threshold Selection Method from Gray-Level Histograms*, *IEEE Transactions on Systems, Man, and Cybernetics*, vol. 9, no. 1, pp. 62-66.